Life Science Informatics Publications
Research Journal of Life Sciences, Bioinformatics, Pharmaceutical and Chemical Sciences
Journal Home page http://www.rjlbpcs.com/
RJLBPCS
ISSN 2454-6348

Original Research Article **DOI: 10.26479/2022.0805.01**

ELUCIDATING VIRULENCE BETWEEN SARS-COV-2 WILD SPIKE PROTEIN AND D614G MUTANT SPIKE PROTEIN USING BIOINFORMATICS

Om Rangacharya*, Alancrita Sudheer, Adesh Temkar, Shrikant Adkine

MIT School of Bioengineering Sciences & Research, MIT Art,

Design and Technology University, Pune, India.

ABSTRACT: The outbreak of novel coronavirus (COVID-19) a contagious acute respiratory syndrome disease, due to its devastating consequences on public health, SARS-CoV-2 has become a major worry worldwide. Due to the mutations and alterations in the genetic material of the Covid-19 virus unable to provide effective treatment to the patients. As a spike mutant of SARS-CoV-2, it was previously recognized as a risk factor for the virus's high fatality rate. In order to infect a host cell, the SARS-CoV-2 attaches to the receptor on that cell and causes the viral and cell membranes to fuse. The functional spike protein integrated into SARS-CoV-2 is enhanced by the D614G mutation, which appears to encourage SARS-CoV-2 transmission in humans. Homology modeling was used to construct both the original spike protein and the D614G mutant spike protein, which was then put through all-atom molecular dynamics simulations. This study will help researchers to determine whether D614G mutant SARS-CoV-2 strains are more virulent than wild-type SARS-CoV-2 strains. Batch docking was used as a part of the drug repurposing technique to locate a medication that was suitable for both wild and mutant spike proteins. Drug Bank was used to identify these antiviral drugs repurposing as well as treatment of covid-19 medications. Using some scoring functions, batch docking assisted us in predicting binding affinities. Understanding the differences in virulence between the SARS-CoV-2 natural spike protein and the D614G mutant spike protein is critical for designing COVID-19 prevention and treatment medicines and vaccines.

Keywords: SARS-CoV-2, homology modeling, D614G, molecular dynamics, molecular docking

Article History: Received: Sept 26, 2022; Revised: Oct 14, 2022; Accepted: Oct 22, 2022.

Corresponding Author: Mr. Om Rangacharya*

MIT School of Bioengineering Sciences & Research, MIT Art, Design and Technology University, Pune, India. Email Address: omrangacharya@gmail.com

1.INTRODUCTION

Coronavirus sickness (COVID-19) is a viral ailment caused by the SARS-CoV-2 virus, which was detected in late 2019 in China. Worldwide, almost 242 million confirmed cases have been recorded. This disease has also proven to be fatal, taking the lives of more than 4.92 million people worldwide. The World Health Organization (WHO) declared a pandemic on March 11 and a Public Health Emergency of International Concern on January 30, 2020 [4]. Infected patients are likely to develop a mild to moderate respiratory disease that goes away without the need for treatment ("Coronavirus Disease (COVID-19) Situation Reports").On the other hand, some can even become critically unwell who require medical assistance. It can make anyone sick and cause a person to get very ill or die at any age [3].COVID-19 is an RNA virus with a single strand of RNA. Coronaviruses are divided into four genera: alphaviruses, beta viruses, gamma viruses, and delta viruses [15]. Bats are the source of alpha- and beta-strains, whereas pigs and birds are the source of gamma- and delta-viruses. The genomic size varies between 26 and 32 kb. It has six to eleven open reading frames (ORFs).The pathogenesis or pathophysiological pathway of potent COVID-19 is still unclear, but includes an uncontrolled hyper-inflammatory response followed by infection [21].Spike protein consists of 2 subunits S1 and S2 who play a vital role individually. S1 helps in mediating binding of the receptor and S2 helps in fusion of downstream membranes. SARS-CoV-2 has been designed to force cell entrance. SARS-CoV binds to ACE2 (metalloprotease), however the SARS-CoV-2 receptor domain is smaller, and acts as well fit for ACE2. The host enzyme furin appears to be used by SARS-COV-2 to remove the viral spike protein [10].The virus has undergone several mutations that make it far more dangerous than other human coronaviruses we have come across so far [20]. This has grabbed up the attention of many scientists for carrying out research on this protein. Coronaviruses are also one of the few RNA viruses with a genomic mutation mechanism that prevents the virus from collecting weakening genetic alterations [13]. Antiviral medications like ribavirin, which prevent viruses like hepatitis C, haven't been able to stop SARS-infected COV-2 from spreading. A proof-reader can eliminate drug-induced mutations that usually weaken viruses [11]. It shows deadly dynamics of action: it often regenerates, modifying and swapping its RNA fragments with other coronaviruses.When the SARS-CoV broke out in 2002-2003, one modification intervened in familiarity with central civet host infection and human transmission.The introduction of D614G, which was uncommon before March 2020 but grew more prevalent as the epidemic expanded, was discovered in SARS-CoV-2 by a sequence analysis of more than 28,000 genes in May 2020. This mutation appeared in more than 74% of all sequences reported in June 2020 [17].D614G, on the other hand, was accompanied by three additional alterations : There is a C-to-T conversion to the 5'uninterrupted region at position 241, a synonymous C-to-T mutation at position 3037, and an unknown C-to-T mutation at position 14408 in the RNA-dependent RNA polymerase

gene8 [17].SG614 pseudotyped retrovirus infects Angiotensin-Converting Enzyme 2(ACE2) cells more efficiently than SD614. This high infectivity was associated with lower S1 molting and greater S-protein insertion into pseudovirion. SG614 does not bind ACE2 in an efficient manner compared to SD614, and pseudo viruses containing these S proteins were counteracted with convalescent plasma of comparable efficiencies. The SG614 virus transmits efficiently [6].In this study, a three dimensional complex structure comprising the D614G mutant spike protein and the wild-type spike protein was built using homology modeling by selecting the mutant spike protein (D614G) of SARS-CoV-2 (PDB ID: 6VYB.1.A) and the Wild type spike protein of SARS-CoV-2 (PDB ID: 6Z97.1.B) using maestro software (Schrodinger) [16].A Ramachandran plot and an Errat plot were used to evaluate the homology models, and the best model was subjected to molecular dynamics simulations [7]. It gave an insight on how the molecules interact and move in a space. Molecular Dynamics trajectories were examined for RMSD (Root Mean Square Deviation) of the backbone of wild and mutant spike proteins [8]. Radius of Gyration, along with RMSF were also studied. As part of the drug repurposing strategy, we also carried out batch docking to find a suitable drug for wild and mutant protein [19].Batch docking helped us to predict binding affinities of different drugs from the library using some scoring functions.

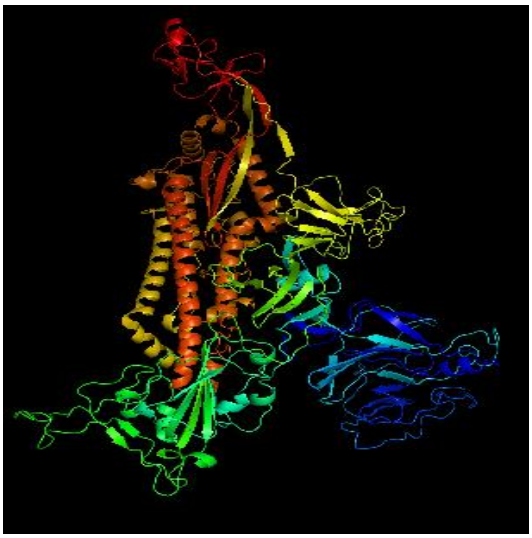

Figure 1. Wild type spike protein of SARS-CoV-2

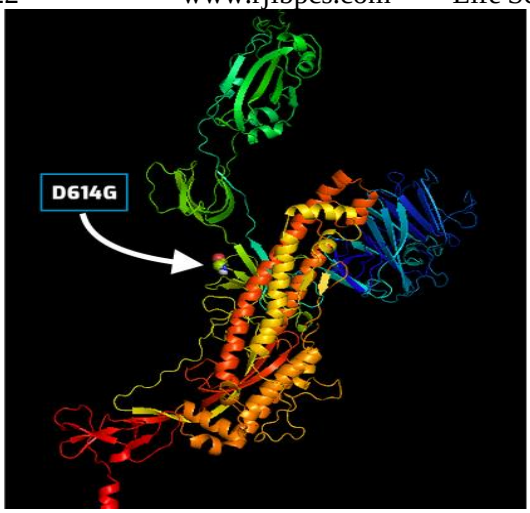

Figure 2. Mutant spike protein of SARS-CoV-2

2. MATERIALS AND METHODS

1. Homology Modeling

The spike protein's sequence was obtained from the RCSB PDB database (https://www.rcsb.org/). The mutant spike protein (D614G) of SARS-CoV-2 (PDB ID: 6VYB.1.A) and the Wild type spike protein of SARS-CoV-2 (PDB ID: 6Z97.1.B) was selected as the template structure. Homology modeling was performed using maestro software (Schrodinger). The DOPE energy value was used to select one of ten models.The selected model's energy was minimized using the Schrödinger suite (www.schrodinger.com) to eliminate steric clashes, and a Ramachandran plot was used to assess the model's stereo-chemical quality [9] and also evaluated to verify the protein structures using the Errat plot.

2. Molecular Dynamics Simulations

Desmond was used to do molecular dynamics simulations utilizing the verified homology model of the Wild type spike protein and Mutant spike protein (D614G) (Schrodinger) [1]. Desmond was used to simulate the stability of wild and mutant spike proteins for 10 ns in molecular dynamics (MD) simulations [2]. Using Desmond's system builder in the Maestro programme, a system for Wild and Mutant proteins was placed inside a water-filled (TIP3P) cubic box with periodic borders and 1 A° spacing.By adding 5 Sodium (NA) ions, the overall charge of the solvent system was neutralized. Over 400 ps from 0 to 300 K, both systems are linearly heated at constant volume (NVT ensemble, 1 bar) [2].Equilibration is accomplished using the Desmond protocol at constant pressure and temperature (NPT ensemble, 300 K, 1 bar) and the Berendsen coupling technique with a one temperature group.The lengths of all hydrogen atom bonds are constrained using M-SHAKE. 10 A° was kept as the cut-off for Van Der Waals and short-range electrostatic interactions.Long-range electrostatic interactions were computed using Particle Mesh Ewald (PME) summation [12].After achieving stability, both systems are put through a 10 ns MD simulation at 300 K and 1 bar of

pressure with no constraints.The equations of motion were integrated using the leap-frog algorithm with a 2 fs time step.Molecular Dynamics trajectories were studied for RMSD of the Backbone of wild and mutant spike proteins, as well as Radius of Gyration and RMSF [1].

3. **Molecular Docking**

Protein preparation

We chose the wild spike protein PDB ID: 6Z97.1.B and D614G spike protein PDB ID: 6VYB of SARS. CoV2. The receptor protein was replaced with polar hydrogen atoms and kollman charges in place of the water molecules that were previously affixed to it. The protein was subsequently transformed into PDBQT format for molecular docking utilizing auto dock tools. In order to calculate docking with a grid-box size of 40 Å × 40 Å × 40Å and a grid spacing of 0.375 Å, Autodock 4.2.6 software was utilized [18].The D614G strain's spike protein was likewise made in the same manner.

Ligand Preparation

We performed molecular dockings with Birinapant, Dynasore, 2-Deoxy-d-glucose (2DG), Leucovorin, Mitoxantrone. We downloaded FDA approved drugs from DrugBank Database (https://go.drugbank.com/) for virtual screening against spike protein wild and mutant. The structures of 2-Deoxy-d-glucose (2-DG), Birinapant, Dynasore, Leucovorin, and Mitoxantrone were retrieved from PubChem's database in sdf format and transformed using the pymol programme into pdb format. The files were stored in the pdbqt format and Gasteiger charges were applied [5].

Receptor-Ligand Docking

The Autodock Vina software was employed to dock receptor-ligands. Receptors and ligands docking was then carried out. Receptor protein was prepared by deleting water molecules and polar hydrogen was added. Then charges were added namely the Kohlman charge. The ligand molecule was saved as pdbqt. The receptor and ligand were stored in pdbqt format and moved to the 'Vina' folder.The receptor and ligand were docked using the grid tools. The configuration and grid dimensions were saved in notepad in ‘txt’ format. Docking was performed on the Vina command prompt. In order to perform docking we called the config file that was saved earlier. After pressing enter, the docking process starts ,the output of which can be seen in the form of poses.The poses were visualized in pymol software [14].

3. RESULTS AND DISCUSSION

3.1 Homology modeling of the spike protein

Homology models were constructed, and DOPE energy values for each homology model were obtained. Models with the lowest dope energy value were chosen as the ideal structure for the spike protein.The Wild Type Spike Protein of Covid 19 crystal structure with (PDB ID-6VSB) has PRO26- ALA67, SER98-VAL143, SER155-MET177, PHE186-SER247, ALA260-PHE329,

ASN334-LYS444, ASN448 - LEU455, PHE 490 - ASN 501, GLY 502 - PRO 621, GLY 639 - SER 673, SER 686 - PRO 812, LYS 814 - ALA 829, ALA 852 - SER 1147 missing residues. Among these missing residues are amino acids from loop regions and the Helix region. The missing residues in helix are LYS304 - PHE338, ASN343 - SER349, TRP353 - SER383, ASP389 - GLY404, ILE410 - GLY416, ASN422 - ASP737, CYS743 - SER758, ALA783 - SER816, ASN824 - THR866, ALA890 - PRO897, GLY910 - GLN913, THR941 - LEU945, SER968 - VAL976, ARG983 - ASP985, VAL1033 - THR1116, ASP1118 - PRO1140, Later on The Mutant protein was modeled by replacing Aspartic acid by glycine at 614th position.A Ramachandran plot and an Errat plot were used to evaluate the models.Fig (3) illustrates, The Ramachandran plot for wild type spike protein indicates that 86.60 percent of residues were in the areas with the most favored regions, 12.10 % were in additional allowed regions, 1.00 % were in generously allowed regions, and 0.30 percent were in disallowed regions. Fig (4) illustrates The Ramachandran plot for mutant type spike protein indicates that 81.60 percent of residues were in the areas with the most favored regions, 16.4 % were in additional allowed regions, 1.2 % were in generously allowed regions, and 0.9 percent were in disallowed regions.Fig (5,6) illustrates, the Errat plot, the Percentage of residues showing error for wild and mutant types was 13.81 and 17.56 % respectively. This result implies that the empirical structures and the homology model were in agreement. As a result, it was employed in subsequent molecular dynamics simulations.

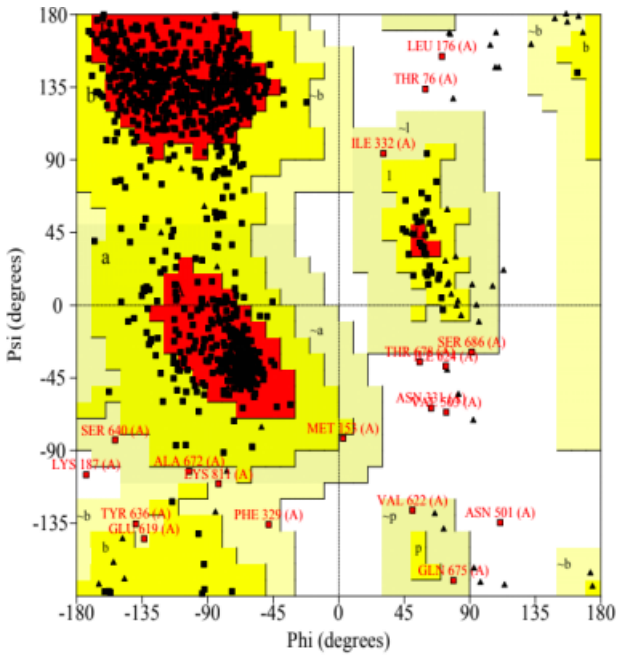

Figure 3. Ramachandran plot for wild type spike protein

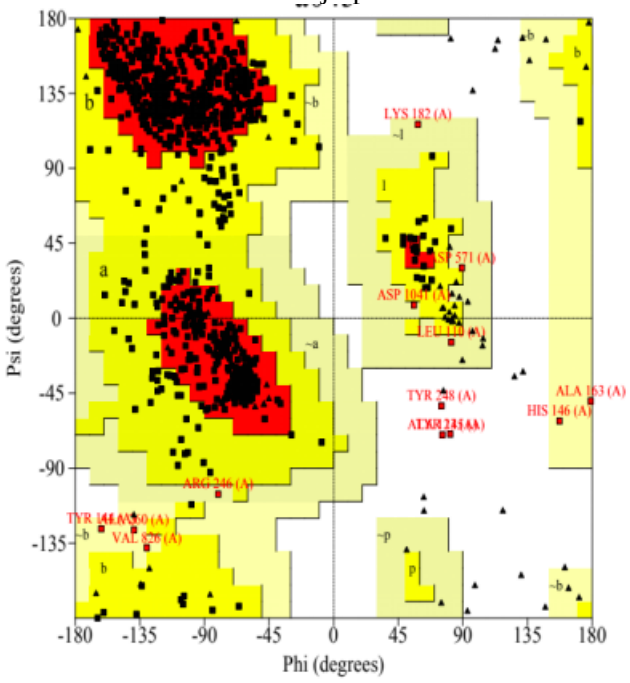

Figure 4. Ramachandran plot for mutant type spike protein

protein

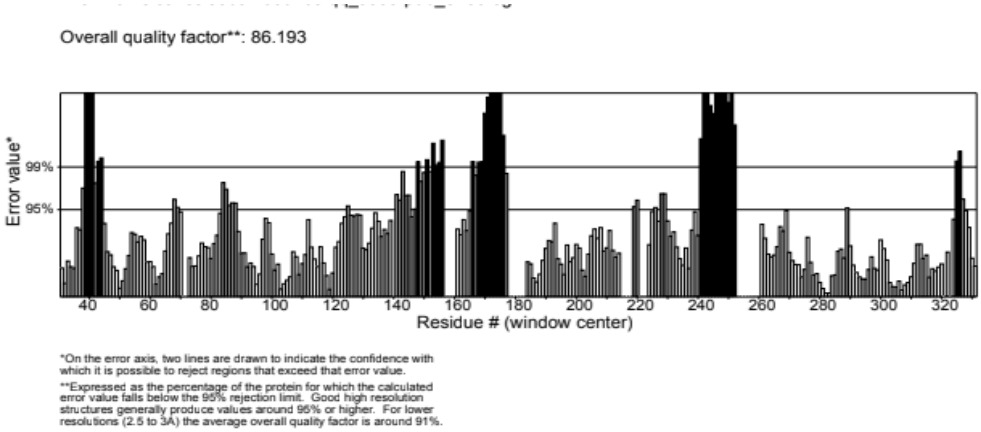

Figure 5. Errat plot for wild type spike protein

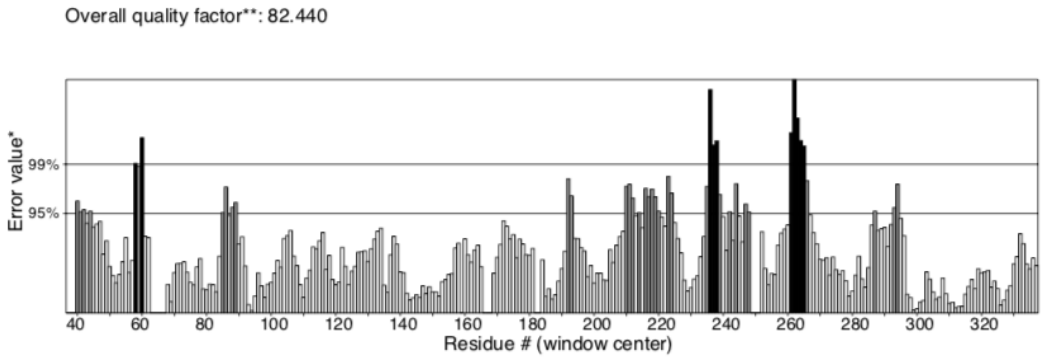

Figure 6. Errat plot for mutant spike protein

3.2 Molecular Dynamics Simulations

To find important residues, the trajectory from molecular dynamics simulations was evaluated. In order to evaluate the stability of the wild type spike protein, mutant spike protein, and fluctuation of residues in simulation.RMSD of C-atoms and RMSF of residues were calculated.Figure (7) : In RMSD vs time plot the wild-type protein was stabilized at 100ps with 10 Å the mutant was stabilized at 200 ps and ranges up to 6ns as an increased phase after 6 ns the mutant protein is completely stabilized till 10 ns. Simultaneously it was noted wild type protein stabilized at 5 ns based on the above results we confirm that the complete water system was properly equilibrated, and neutralized further investigation was carried out for the fluctuations of backbone to understand the role of specific amino acids for the stability of the protein.

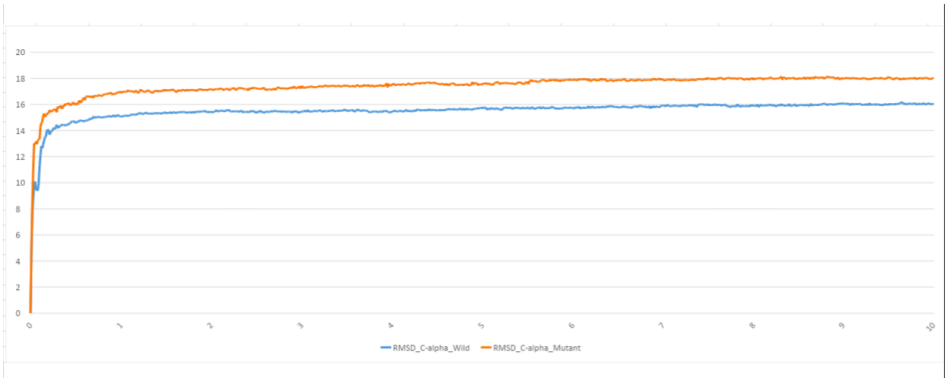

Figure 7. Root mean square deviation (RMSD) plot for the Severe Acute Respiratory Syndrome Coronavirus-2 Wild type spike protein and Mutant spike protein (D614G) during the 10 ns molecular dynamics simulations. The X-axis indicates the time in ns and the Y-axis represents RMSD values in Å.

Figure (8): This numerical measurement is comparable to RMSD, except RMSF calculates individual residue flexibility, or how much a specific residue fluctuates throughout a simulation, as

opposed to identifying positional changes across complete structures over time. The most structurally important amino acids in a protein that contribute the most to molecular motion can be identified by plotting the RMSF per residue vs. the residue number. Higher RMSF values are most typically seen in loop areas with more conformational flexibility and less well defined structuresRMSF graph illustrating MD for 10 ns of Wild and Mutant type D614G Spike protein, with X-axis indicating residues and Y-axis representing RMSF (nm). In that mutant type shows higher variation than Wild type. Given the complexity of each protein's nature, flexibility in the structure is essential to maintaining the dynamics of the protein. The RMSF was calculated in order to gauge how flexible the wild-type and mutant protein structures are.The RMSF values were lower for the helix and sheets, but they were larger for twists and bends. In comparison to wild protein, the D614G mutant exhibits larger variations in a number of areas.The total RMSF for both the wild-type and mutant proteins was calculated. The mutant protein had larger variations than other proteins between residues 668–680, 793–799, 1014–1030,1035–1044,and1054–1086

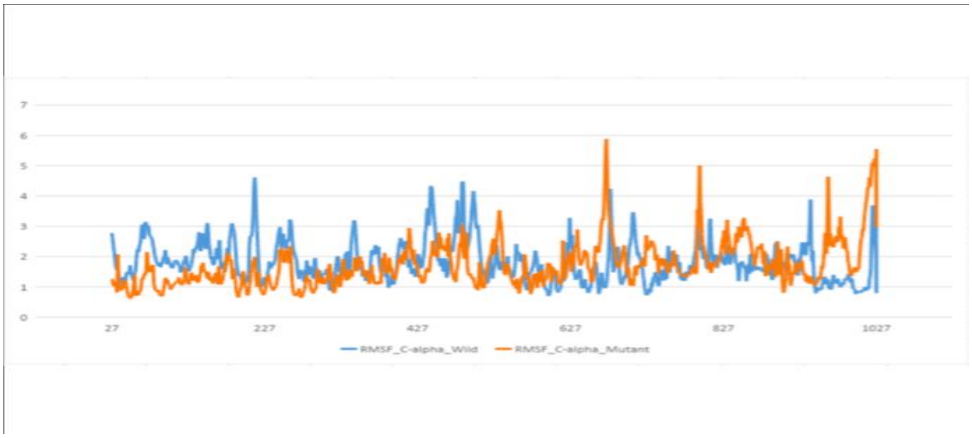

Figure 8. The Root Mean Square Fluctuation (RMSF) plot for Cα atoms of the Severe Acute Respiratory Syndrome Coronavirus-2 Wild spike protein and Mutant spike protein (D614G) during the 10 ns molecular dynamics simulations. The X-axis indicates residue number and Y-axis represents the RMSF value in Å

Compactness of protein during MD simulation is measured by Radius of gyration (RoG). Initially the wild protein model might have lost binding which is predicted by higher Rg value of 44.5 nm. Furthermore, Rg value gradually decreases to 30.5 nm which may be due to adjustment of force of interaction within the structure and resulting in making a more compact structure. Simulation period between 5-6ns there is a lot of variation - an increase and constant Rg value of 34nm. After reaching 6ns, there is a decrease in compression which increases its interaction with other molecules but reduces its stability. But, at 10 ns a sudden increase in Rg value can be seen.Mutant protein model lost binding at 45.5 nm which is understood by its higher Rg value. Rg value keeps declining till 30.5nm which is due to force of interaction adjustment within the structure. This resulted in a more

compact structure. At the 5.5 ns -6ns simulation period, there is little variation in graphs which show increase in compression in the vicinity of the mutant if higher than wild protein. This reduces interaction of mutant with other molecules & increases its stability.

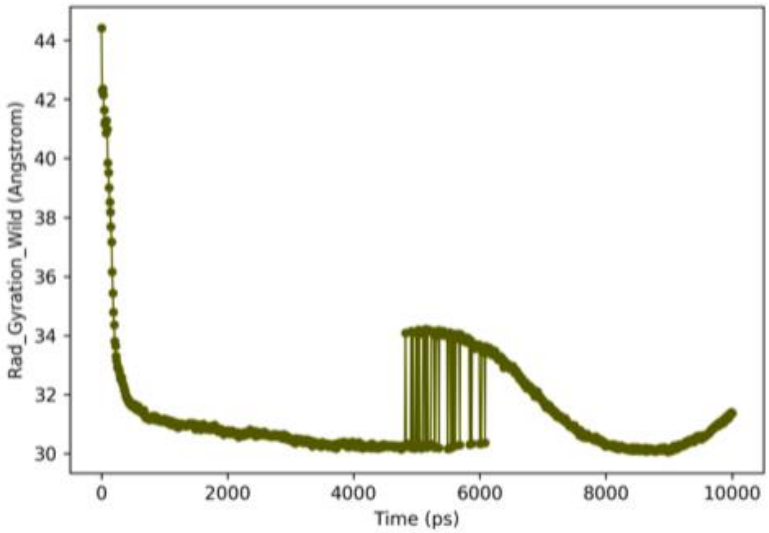

Figure 9. The Radius of Gyration (RoG) plot of the Severe Acute Respiratory Syndrome Coronavirus-2 Wild spike protein during the 10 ns molecular dynamics simulations. The X-axis indicates Time(ps) and Yaxis represents the RoG value in Å

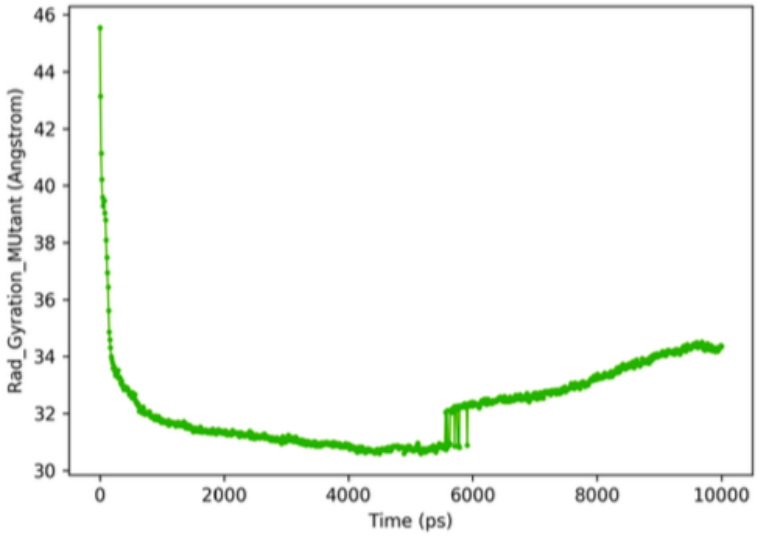

Figure 10. The Radius of Gyration (RoG) plot of the Severe Acute Respiratory Syndrome Coronavirus-2 Mutant spike protein during the 10 ns molecular dynamics simulations. The X-axis indicates Time(ps) and Yaxis represents the RoG value in Å

3.3 Molecular Docking

In this present study, molecular dockings were carried out with Mitoxantrone, Leucovorin, 2DG, Dynasore, and Birinapant (Known Anti-covid drugs).To see how these punctual mutations influence protein-ligand binding inhibitors on the mutant and wild spike protein of SARS-CoV-2.In vitro studies have demonstrated that the drug mitoxantrone prevents SARS-CoV-2 infection. As a result, we chose Mitoxantrone for docking with WT spike protein and mutations in this work.Mitoxantrone forms a conventional hydrogen bond with THR (A: 961), ALA(A:958) and ARG(A:1014), and Sigma and pi bond with THR (A:1006) and pi-alkyl interactions with LEU(A:962) in the WT complex.Mitoxantrone has binding free energy (-5.6 kcal/mol) when bound to WT spike protein, followed by the D614G mutant (- 6.0 kcal/mol) that form a hydrogen bond with GLN (A: 321), VAL(A:622), TYR(A:612) residues.

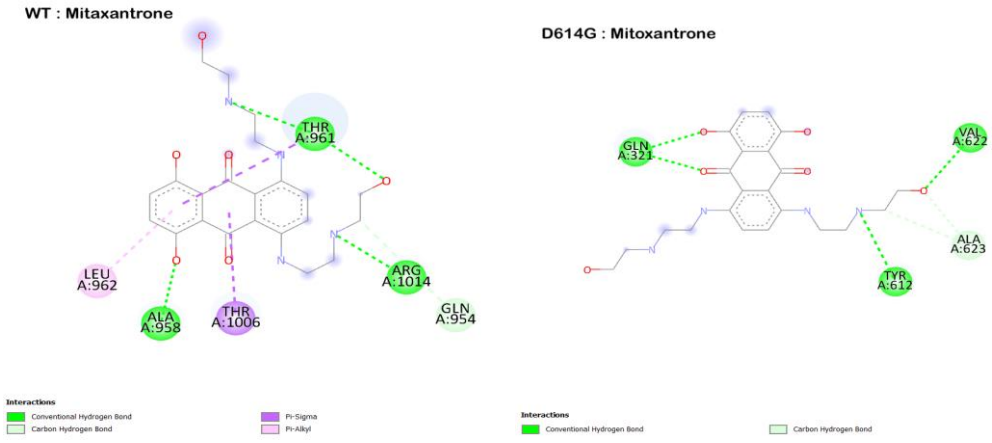

(a) (b)

Figure 11. (a) Binding pose of Mitoxantrone within the WT spike protein binding pocket, (b) Binding pose of Mitoxantrone within the D614G mutant protein binding pocket

In several cancer cells, leucovorin has been demonstrated to be a promising antagonist. According to our findings. Leucovorin forms solely hydrogen bonds with SARS-CoV-2. It forms a conventional hydrogen bond with SER (A:45), ASN(A:856) and ARG(A:1000), and Sigma and pi bond with ALA (A:852) and pi-alkyl interactions with LEU(A:966) in WT complex. Leucovorin can also inhibit SARS-CoV-2, as evidenced by its binding energy of -6.5 kcal/mol.Whereas in D614G it has a binding energy of -6.8 kcal/mol.D614G S protein interacts with leucovorin via establishing hydrogen bonds between the compound and the amino acids SER (A:50), CYS(A:301),

LYS(A:304), and HIS (A:625). It also forms pi-alkyl interactions with CYS(A:291) ALA (A:292), PRO(A:295). We also observed Pi-Anion interaction with residue GLU (A:298).

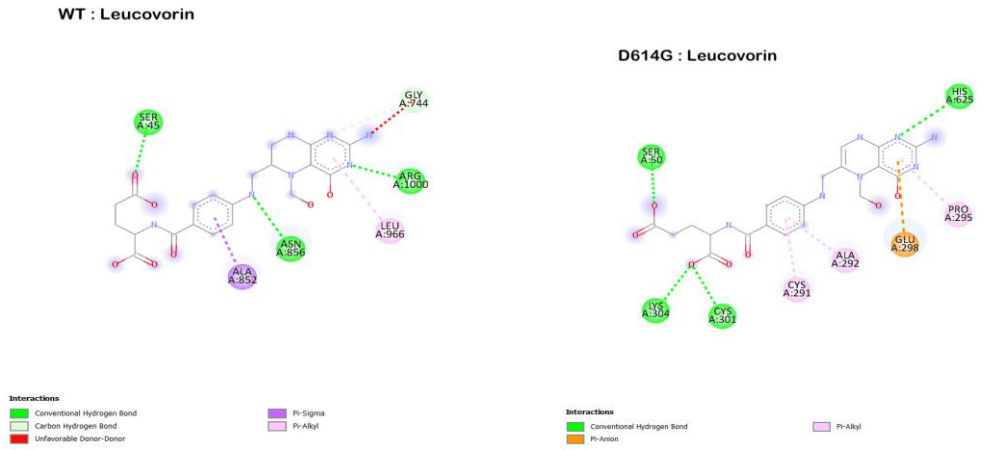

a. (b)

Figure 12. (a) Binding pose of leucovorin within the WT spike protein binding pocket, (b) Binding pose of leucovorin within the D614G mutant protein binding pocket

In cooperation with Dr. Reddy's lab, the Defense Research and Development Organization (DRDO) introduced the anti-Covid-19 drug 2-Deoxy-D-Glucose. The abbreviation 2-DG stands for 2-Deoxy-D-Glucose. As a result, 2-DG was tested using molecular docking against the WT and mutant version of the S protein. 2-DG bound to WT S protein with the binding free energy (-5.1 kcal/mol), followed by D614G (-5.3 kcal/mol). 2-DG interacted with the WT spike protein, forming a hydrogen bond with the amino acids GLN (A:965) and (A:1014).

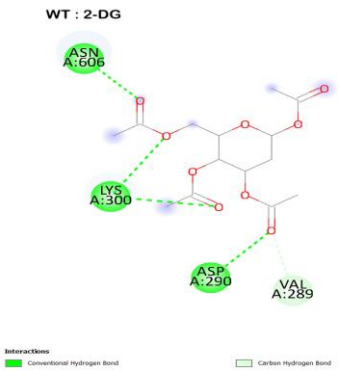

Figure 13. (a) Binding pose of 2-DG within the WT spike protein binding pocket

Mutant forms hydrogen bonds with Birinapant and Dynasore, both antiviral drugs, have a high binding affinity for SARS-CoV-2 spike protein. (Shaimaa A. Gouhar, 2021) Birinapant forms one conventional hydrogen bond with ARG(A:44), carbon hydrogen bond with SER(A:50) and halogen bond with LEU (A:48). It also formed Pi cation LYS (964) , Pi-Sigma VAL(A:47) as well as pi-alkyl interaction with ALA(A:852) in WT complex.In Mutant it forms hydrogen bond with TYR

(A:612) , pi-alkyl interactions with ILE(A:624) ALA (A:292),Pi sigma bond with ARG (A:319)and Pi anion GLU(298).We also observed Van der Waals interaction with residue VAL (A:320). In the WT complex Birinapant has binding energy of -8.3 kcal/mol and in D614G binding energy of -8.2 kcal/mol.

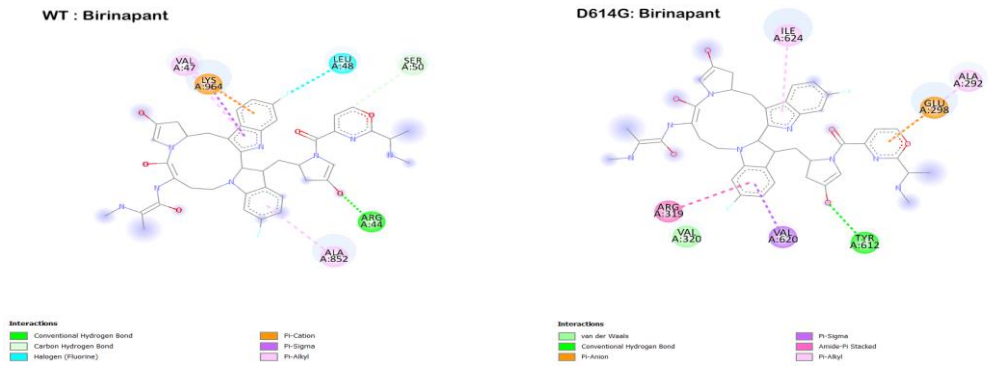

(a) (b)

Figure 14. (a) Binding pose of Birinapant within the WT spike protein binding pocket, (b) Binding pose of Birinapant within the D614G mutant protein binding pocket

In WT and mutant complexes, Dynasore shows binding energy of -7.4 and -7.2 kcal/mol respectively. In WT it forms three hydrogen bonds ARG(A:1014) GLN (A:1010), GLN(A:954) and one carbon hydrogen bond with GLN (A:957). It also forms Pi-sigma THR(A:961) and Pi-alkyl bond with ALA(A:958).In Mutant complex Dynasore formed two hydrogen bonds HIS(A:625) and TYR(A:612), three pi-alkyl bond VAL(A:620) , ILE(A:624) , VAL(A:320) and one pi-anion interaction with GLU(A:298)residue.

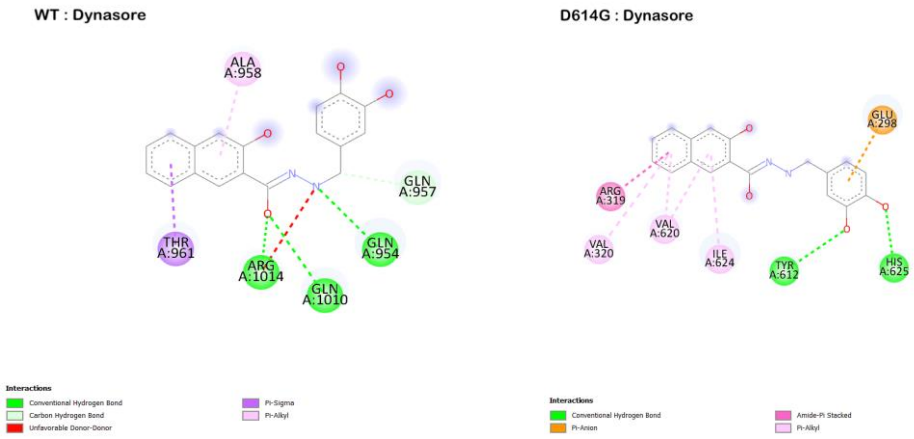

(a) (b)

Figure 15. (a) Binding pose of Dynasore within the WT spike protein binding pocket, (b) Binding pose of Dynasore within the D614G mutant protein binding pocket.

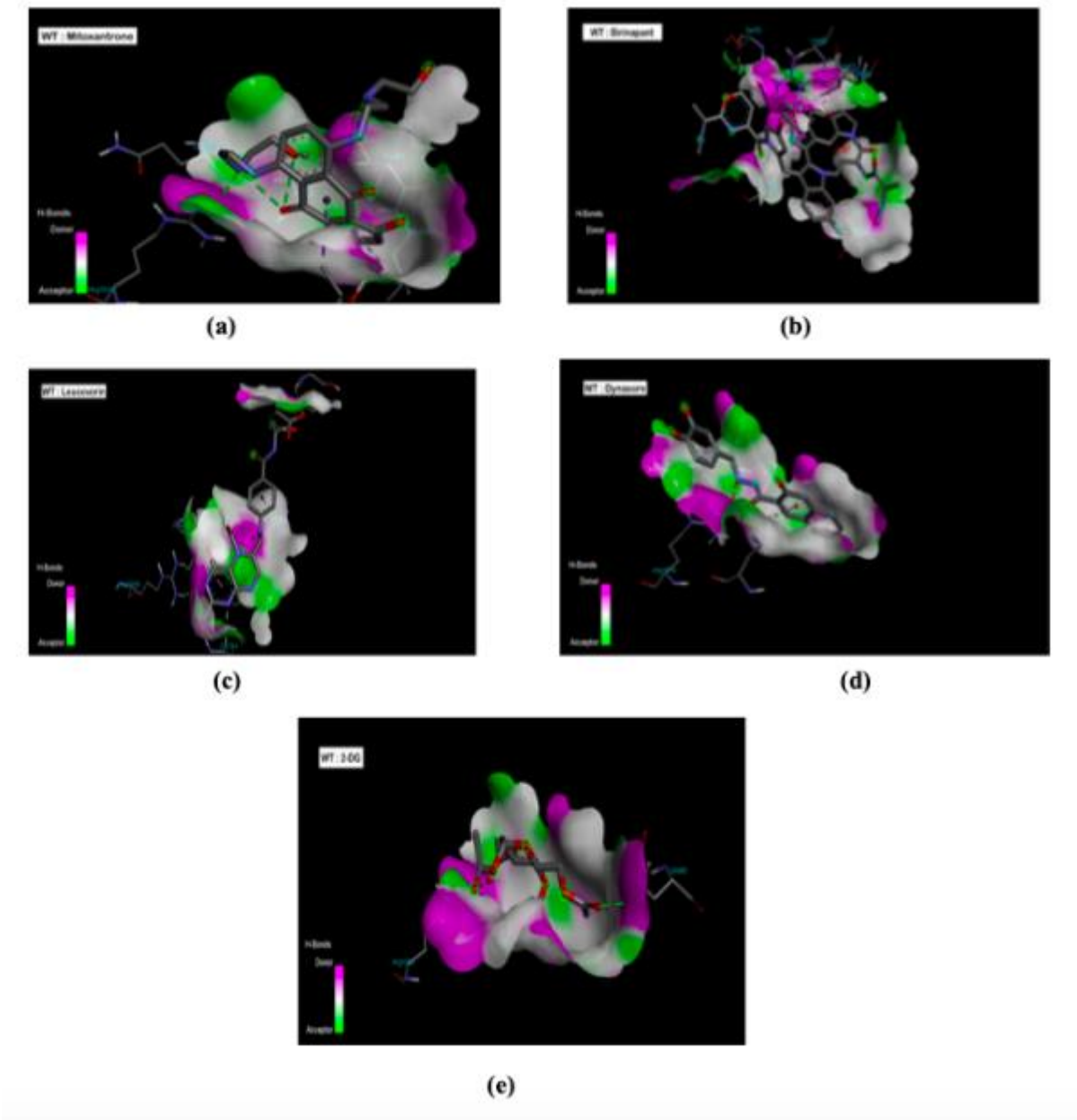

Figure 16. Protein - drug interaction is shown as a surface 3D binding cavity. Protein is wild type spike protein and drug that is interacting with it are as follows: (a) Mitoxantrone, (b) Birinapant, (c) Leucovorin, (d) Dynasore and (e) 2-DG

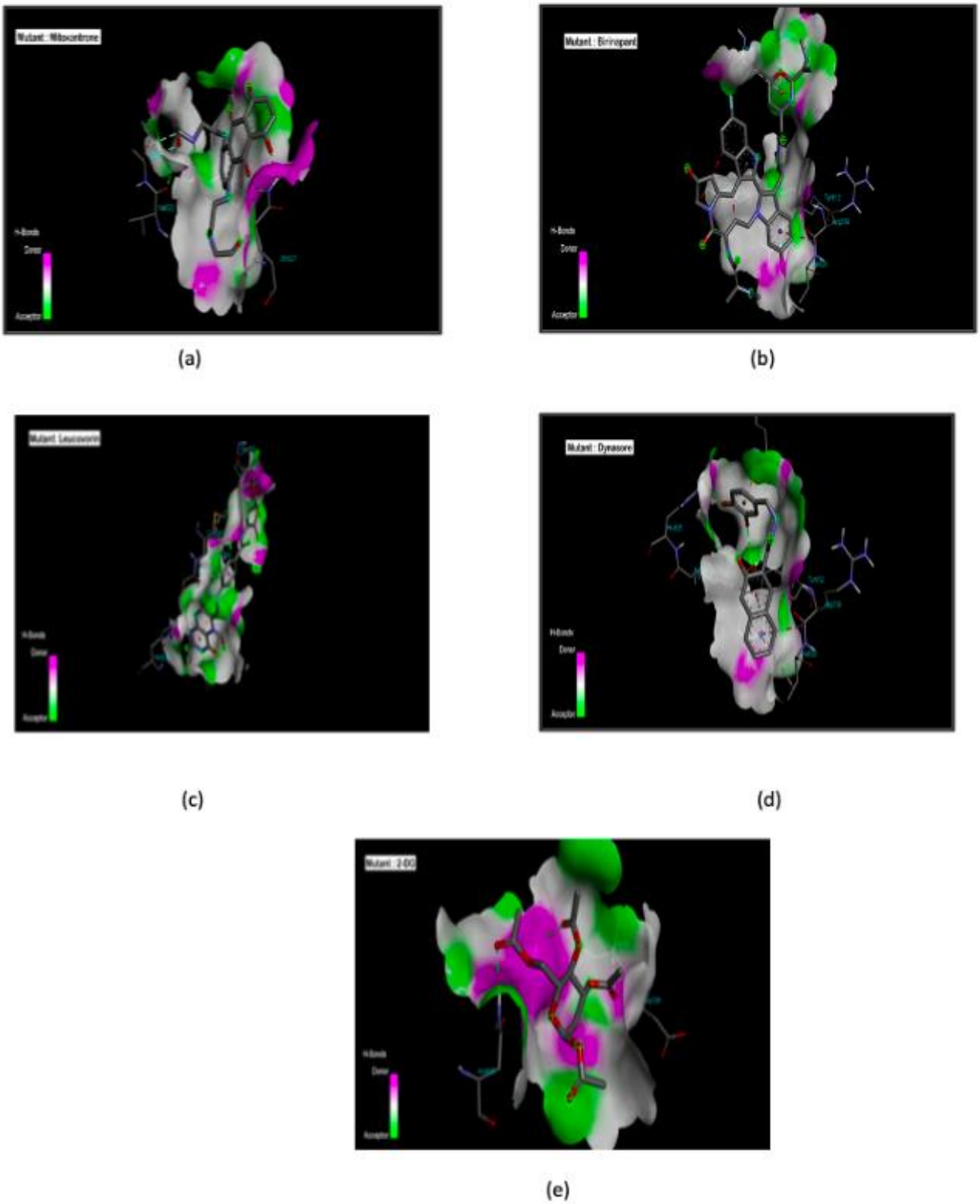

Figure 17. Protein - drug interaction is shown as a surface 3D binding cavity. Protein is a D614G mutant and drug that is interacting with it are as follows: (a) Mitoxantrone, (b) Birinapant, (c) Leucovorin, (d) Dynasore and (e) 2-DG.

3.4 Hydrogen Bond Interactions

Hydrogen bonds are major interactions between proteins. Hence, Maestro was used to identify hydrogen bonds produced between wild spike protein and mutant spike protein in the typical structure using molecular dynamics simulations.Figure (18) and (19) show how the amount of hydrogen bonds changes during the course of the simulation.In the case of the mutant protein, the number of hydrogen bonds was maintained during simulation to a certain extent.While in case of wild proteins, H bonds keep on increasing.From Fig (18), we can observe drastic loss of intermolecular interaction from 7000 ps - 10,000s. This wave is missing in the plot of mutation simulation. This is the result of a non-deterministic simulation process which is probably caused by mutation.In Fig (19)The formation of H-Bonds started from 1175 to 1250 in 0ps. After having a great rapid forming it comes to the Log phase 1250 to 1315 in 0 – 7000ps then comes the lag phase from 1275 to 1365 in 6000 -10000ps here the Peak is high.In Fig (19) at one point there is a rapid formation of H-bonds from 1140 to 1220 in 0 – 2000ps. After having a great rapid forming it comes to the stationary Phase from 1240 to 1270 in during the 10ns. In between there is a high mutation peak of H-bonds at 1295 at 9000ps and the lowest mutation peak at 1200 in 1000ps below the stationary phase.

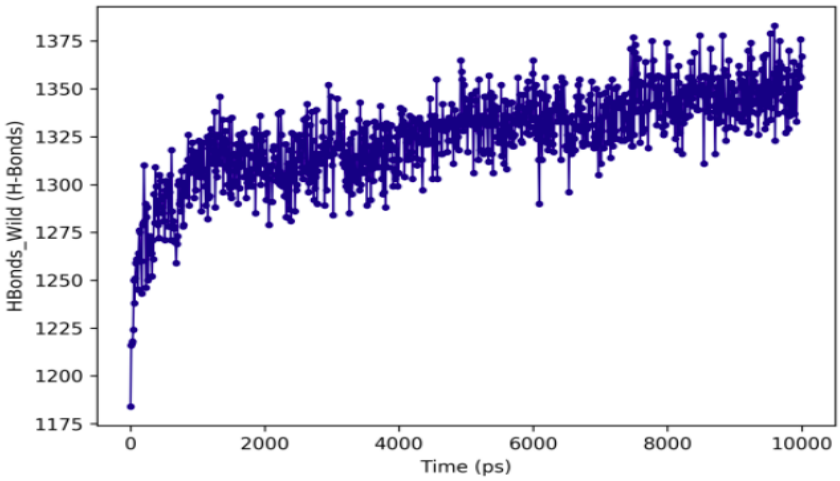

Figure 18. Hydrogen bond interaction for Wild type spike protein of Severe Acute Respiratory Syndrome Coronavirus-2

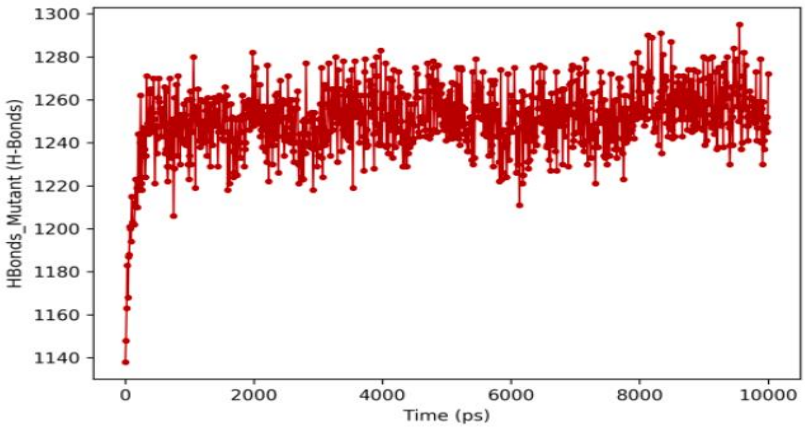

Figure 19. Hydrogen bond interaction for Mutant spike protein (D614G) of Severe Acute Respiratory Syndrome Coronavirus-2

4. CONCLUSION

Homology modeling was used to create the structures of the wild-type and mutant spike proteins (D614G). According to evaluations using the Ramachandran plot and Errat Plot, the homology model was of high quality.Further, To find important residues at 10 ns, the trajectory from molecular dynamics simulations was evaluated. RMSD of CÂ atoms and RMSF of residues were used to investigate the stability and fluctuation of the mutant and wild type spike protein. Protein compactness was also assessed using the radius of gyration. At the 5.5-6ns simulation period, there is little variation; an increase in graphs which show increase in compression in the vicinity of the mutant is higher than wild protein. This reduces interaction of mutant with other molecules & increases its stability. It may be easier to create medications and vaccines to prevent SARS-CoV-2 infection and to fight COVID-19 as a result of the new insights this work offers into the processes of SARS-CoV-2 infection.

ETHICS APPROVAL AND CONSENT TO PARTICIPATE

Not applicable.

HUMAN AND ANIMAL RIGHTS

No Animals/Humans were used for studies that are base of this research.

CONSENT FOR PUBLICATION

Not applicable.

AVAILABILITY OF DATA AND MATERIALS

The author confirms that the data supporting the findings of this research are available within the article.

FUNDING

None.

ACKNOWLEDGEMENT

The authors would like to thank the Drug Discovery Hackathon (DDH2020), a joint initiative of CSIR and AICTE who gave us a chance to do our research work. We express our sincere gratitude to the Government of India for allowing the utilization of CDAC servers. It helped in the optimization of the supercomputer for Docking and Dynamic calculations. We offer our sincere appreciation for the learning opportunities provided by NIC, MyGov, and the Office of Principal Scientific Advisor.Finally, everything became possible due to the tireless efforts of the team.

CONFLICT OF INTEREST

The authors have no conflict of interest.

REFERENCES

1. Bhattarai N, Baral P, Gerstman BS, Chapagain PP. Structural and dynamical differences in the spike protein RBD in the SARS-CoV-2 variants B. 1.1. 7 and B. 1.351. The Journal of Physical Chemistry B. 2021 Jun 10;125(26):7101-7.
2. Bowers KJ, Chow E, Xu H, Dror RO, Eastwood MP, Gregersen BA, Klepeis JL, Kolossvary I, Moraes MA, Sacerdoti FD, Salmon JK. Scalable algorithms for molecular dynamics simulations on commodity clusters. InProceedings of the 2006 ACM/IEEE Conference on Supercomputing 2006 Nov 11 (pp. 84-es).
3. Ciotti M, Ciccozzi M, Terrinoni A, Jiang WC, Wang CB, Bernardini S. The COVID-19 pandemic. Critical reviews in clinical laboratory sciences. 2020 Aug 17;57(6):365-88.
4. Cucinotta D, Vanelli M. WHO declares COVID-19 a pandemic. Acta Bio Medica: Atenei Parmensis. 2020;91(1):157.
5. Djokovic N, Ruzic D, Djikic T, Cvijic S, Ignjatovic J, Ibric S, Baralic K, Buha Djordjevic A, Curcic M, Djukic-Cosic D, Nikolic K. An Integrative in silico Drug Repurposing Approach for Identification of Potential Inhibitors of SARS-CoV-2 Main Protease. Molecular Informatics. 2021 May;40(5):2000187.
6. Fernández A. Structural impact of mutation D614G in SARS-CoV-2 spike protein: enhanced infectivity and therapeutic opportunity. ACS medicinal chemistry letters. 2020 Aug 17;11(9):1667-70.
7. Hollingsworth SA, Karplus PA. A fresh look at the Ramachandran plot and the occurrence of standard structures in proteins.
8. Kumar R, Kumar R, Goel H, Tanwar P. Computational investigation reveals that the mutant strains of SARS-CoV2 have differential structural and binding properties. Computer Methods and Programs in Biomedicine. 2022 Mar 1;215:106594.
9. Laskowski RA. PDBsum: summaries and analyses of PDB structures. Nucleic acids research. 2001 Jan 1;29(1):221-2.

10. Li F. Structure, function, and evolution of coronavirus spike proteins. Annual review of virology. 2016 Sep 29;3(1):237.
11. Martinez MA. Lack of effectiveness of repurposed drugs for COVID-19 treatment. Frontiers in Immunology. 2021 Mar 11;12:635371.
12. Messias A, Santos DE, Pontes FJ, Lima FS, Soares TA. Out of sight, out of mind: The effect of the equilibration protocol on the structural ensembles of charged glycolipid bilayers. Molecules. 2020 Nov 4;25(21):5120.
13. Na W, Moon H, Song D. A comprehensive review of SARS-CoV-2 genetic mutations and lessons from animal coronavirus recombination in one health perspective. Journal of Microbiology. 2021 Mar;59(3):332-40.
14. Narkhede RR, Cheke RS, Ambhore JP, Shinde SD. The molecular docking study of potential drug candidates showing anti-COVID-19 activity by exploring of therapeutic targets of SARS-CoV-2. Eurasian Journal of Medicine and Oncology. 2020 Apr 29;4(3):185-95.
15. Pal M, Berhanu G, Desalegn C, Kandi V. Severe acute respiratory syndrome coronavirus-2 (SARS-CoV-2): an update. Cureus. 2020 Mar 26;12(3).
16. Pitman MR, Menz RI. Methods for protein homology modelling. InApplied mycology and biotechnology 2006 Jan 1 (Vol. 6, pp. 37-59). Elsevier.
17. Plante JA, Liu Y, Liu J, Xia H, Johnson BA, Lokugamage KG, Zhang X, Muruato AE, Zou J, Fontes-Garfias CR, Mirchandani D. Spike mutation D614G alters SARS-CoV-2 fitness. Nature. 2021 Apr;592(7852):116-21.
18. Seeliger D, de Groot BL. Ligand docking and binding site analysis with PyMOL and Autodock/Vina. Journal of computer-aided molecular design. 2010 May;24(5):417-22.
19. Vardhan S, Sahoo SK. Searching inhibitors for three important proteins of COVID-19 through molecular docking studies. arXiv preprint arXiv:2004.08095. 2020 Apr 17.
20. World Health Organization. SARS-CoV-2 Evolution [Internet]. www.who.int. 2020. Available from: https://www.who.int/news-room/questions-and-answers/item/sars-cov-2-evolution
21. Yuki K, Fujiogi M, Koutsogiannaki S. COVID-19 pathophysiology: A review. Clinical immunology. 2020 Jun 1;215:108427.